GSK2556286 is a novel antitubercular drug candidate effective in vivo with the potential to shorten tuberculosis treatment

Authors:

Eric L. Nuermberger [1*], Maria Santos Martínez-Martínez[2], Olalla Sanz[2], Beatriz Urones[2], Jorge Esquivias[2], Heena Soni[1], Rokeya Tasneen[1], Sandeep Tyagi[1], Si-Yang Li[1], Paul J. Converse[1], Helena I. Boshoff [3], Gregory T Robertson[4], Gurdyal S Besra[5], Katherine A. Abrahams[5], Anna M Upton[6b], Khisimuzi Mdluli[6,c], Gary W Boyle[7], Sam Turner[7], Nader Fotouhi[6], Nicholas C. Cammack[2d], , Juan Miguel Siles[2], Marta Alonso[2], Jaime Escribano[2], Joel Lelievre[2], , Esther Pérez-Herrán[2], Robert H. Bates[2], Gareth Maher-Ewards[4], David Barros[2], Lluís Ballell[2,a], Elena Jiménez[2*]

Affiliations:

1. JHU: Center for Tuberculosis Research, Division of Infectious Diseases, Johns Hopkins University School of Medicine, Baltimore, Maryland, United States of America
2. GSK: Diseases of the Developing World, GlaxoSmithKline R+D Limited, Parque Tecnológico de Madrid, Calle de Severo Ochoa, 2, 28760 Tres Cantos, Madrid, Spain.
3. Tuberculosis Research Section, Laboratory of Clinical Immunology and Microbiology, National Institute of Allergy and Infectious Diseases (NIAID), National Institutes of Health (NIH), Bethesda, MD 20892, USA
4. Mycobacteria Research Laboratories, Department of Microbiology, Immunology and Pathology, Colorado State University, Fort Collins, Colorado, United States of America IPK: Institut Pasteur Korea, Sampyeong-dong, Seongnam-si, Gyeonggi-do, Korea

5. Institute of Microbiology and Infection, School of Biosciences, University of Birmingham, Birmingham B15 2TT, U.K.6. GSK: Research, GlaxoSmithKline R&D, Ware, UK.

6. TB Alliance: Global Alliance for Tuberculosis Drug Development, New York, NY 10005

7. GSK: Research, GlaxoSmithKline R&D, Ware, UK.

Current affiliations:

[a] Global Public Health Janssen R&D. Beerse, Belgium

[b] Evotec Inc, (US) Princeton, NJ 08540

[c] Bill & Melinda Gates Medical Research Institute, One Kendall Square, Building 600, Suite 6-301, Cambridge, MA 02139

[d] Wellcome Trust

Running Title: Novel drug GSK2556286 shortens treatment in murine TB

*To whom correspondence should be addressed: elena.n.jimenez@gsk.com, enuermb@jhmi.edu

One Sentence Summary: GSK2556286 is a novel preclinical drug candidate for the treatment of tuberculosis with a new mode of action potentially able to contribute to the shortening of TB chemotherapy.

Abstract: As a result of a high-throughput compound screening campaign of *Mycobacterium tuberculosis* infected macrophages, a new preclinical drug candidate for the treatment of tuberculosis has been identified. GSK2556286 inhibits growth within human macrophages (IC_{50} = 0.07 μM), is active against extracellular bacteria in cholesterol-containing culture media and exhibits no cross-resistance with known antitubercular drugs. In addition, it has shown efficacy in different mouse models of tuberculosis (TB) and has an adequate safety profile in two preclinical species. These features indicate a compound with a novel mode of action, although still not fully defined, that is effective against both multidrug or extensively-resistant (M/XDR) and drug-sensitive (DS) *M. tuberculosis* with the potential to shorten the duration of treatment in novel combination drug regimens.

Introduction

According to World Health Organization (WHO) estimates for 2019, 10 million people were newly diagnosed with tuberculosis (TB) and 1.4 million died (1), making TB the single greatest cause of death globally by a single infectious agent prior to the COVID-19 pandemic. Multidrug-resistant TB (MDR-TB) threatens TB control in many countries with approximately 363,000 new cases globally in 2019 (1). Furthermore, the incidence of extensively drug-resistant TB (XDR-TB), defined as MDR-TB plus resistance to at least one second-line injectable drug (e.g., amikacin, kanamycin or capreomycin) and a fluoroquinolone, was over 12,000 in 2019. Cases of XDR-TB have now been reported in over 100 countries (1). Despite regulatory approvals for bedaquiline (B), delamanid (D) and pretomanid (Pa) in the past decade to treat MDR or XDR-TB, there remains an unmet need for novel drugs with new mechanisms of action that are effective against drug-susceptible and drug-resistant forms of TB and shorten the duration of treatment required to prevent relapse.

To date, virtually all approved drugs used to treat TB were identified through phenotypic screens against actively replicating *Mycobacterium tuberculosis* in artificial nutrient-rich media, or they were repurposed from other infectious indications (2). The first-line TB drug pyrazinamide (Z) is the notable exception, having been identified by screening for activity in a murine TB model (3, 4). Few other pathogens rival *M. tuberculosis* in their ability to adapt to and persist within the infected host. Alternative screening methodologies that better represent the environmental conditions and stresses encountered by *M. tuberculosis* within the host have gained favor in recent years and may increase the efficiency with which new molecules with novel sterilizing activity are identified to complement existing TB drugs (5).

Over the last decade, we and others hypothesized that the macrophage, as a primary target of infection by *M. tuberculosis* and a niche in which the pathogen persists in established lesions, might represent an improved surrogate model to facilitate the discovery of novel TB drugs (6, 7). The cytochrome bc_1:aa_3 complex inhibitor telacebec is the first TB drug to reach clinical trials that was initially identified in a phenotypic high-content screening approach using a macrophage infection model (7, 8). Nonetheless, it is active against *M. tuberculosis* in standard nutrient-rich media as well as in macrophages. More recently, novel compounds with selective activity within macrophages were identified and shown to have cholesterol-dependent activity against extracellular *M. tuberculosis in vitro* (9). Previous observations suggest that cholesterol uptake and utilization is essential for pathogen survival in the host and indicate these pathways as potential targets for novel TB drugs (10, 11) Despite these encouraging results, no molecule identified as having such macrophage-specific, cholesterol-dependent activity *in vitro* has progressed to clinical proof-of-concept studies. Here, we describe the discovery of GSK2556286, a novel inhibitor of *M. tuberculosis* extracellularly in the presence of cholesterol and within human macrophages, that provides evidence of favorable *in vivo*

efficacy and safety profiles justifying further development as an attractive companion drug with the potential to shorten the duration of treatment in novel combination regimens for drug-susceptible and drug-resistant TB.

Results

Microbiological profile

To identify compounds that effectively inhibit intracellular growth of *M. tuberculosis*, we screened a library of compounds against bacteria residing within human (THP-1) macrophage-like differentiated monocytes. The exploitation of this screening approach led to the identification of GSK2556286 (Fig. 1), a compound with potent activity (Table 1) against *M. tuberculosis* inside infected macrophages (lC_{50}=0.07 μM in THP-l cells) and the unusual phenotype of requiring the presence of cholesterol to demonstrate activity in axenic culture (IC_{50}=0.71-2.12 μM). The maximal % inhibition of growth achieved by GSK2556286 in these studies was 86% (range 62 to 89.4%).

Table 1. *In vitro* activity of GSK2556286 under various conditions

Compound	IC_{50} (μM) against *M. tuberculosis* strains H37Rv or Erdman				
	Intracellular activity	Extracellular activity			
	H37Rv in THP-1 cells	H37Rv in glucose media	H37Rv in cholesterol media	Erdman in glucose media	Erdman in cholesterol media
GSK2556286	0.07	> 125	2.12	> 50	0.71
Rifampicin	0.0008	0.15	0.2	0.1	0.1
Moxifloxacin	0.16	0.11	0.5	0.28	0.4

GSK2556286 displayed consistent *in vitro* activity in the presence of cholesterol against a panel of clinical isolates with varying drug resistance phenotypes, including isolates from MDR and XDR-TB cases (Supplemental Table S1). The minimal inhibitory concentration of GSK2556286 that inhibited the growth of at least 90% of isolates (MIC90) was determined for 45 clinical isolates (from the National Institute of Health [NIH]), plus 3 laboratory strains, with different resistance phenotypes, including DS, MDR, XDR or other resistance phenotypes (Supplemental Table S2) as well as two additional species belonging to the *M. tuberculosis* complex, *Mycobacterium africanum (M. africanum)* and *Mycobacterium bovis (M. bovis)* in order to evaluate the activity of GSK2556286 on more genetically diverse species of the complex.

The MIC90 was 1.2 µM (MIC range 0.3 to 1.4 µM) similar to that determined for laboratory strains, Erdman and H37Rv (0.71 and 2.12 µM, respectively) in cholesterol containing media.

To investigate the potential mode of action, we isolated spontaneous resistant mutants to GSK2556286 when *M. tuberculosis* Erdman cultivated *in vitro* or extracted from the lungs of infected C3HeB/FeJ mice exposed to GSK2556286 at 96 µM (8xMIC in solid media including cholesterol). In total, 29 colonies isolated from GSK2556286-containing plates in the *in vitro* and *in vivo* experiments were serially passaged on GSK2556286-containing plates and confirmed to have IC_{90} values in the presence of cholesterol that were 10-fold higher than the wild-type parent. Whole genome sequencing and further analysis revealed that 14 out of 29 mutants had mutations mapping to the *Rv1625c* gene (*cya*) (Supplemental Table S3), which encodes a Class IIIa membrane-anchored adenylyl cyclase that is non-essential for growth under routine *in vitro* conditions and has been implicated in resistance to other compounds with cholesterol-dependent activity (9). The remainder of isolated resistant mutants remain under analysis to identify new mutations responsible of resistance.

None of the isolated resistant mutants, with *cya* mutation, had a complete deletion of the *cya* gene. Therefore, a *cya* knock-out mutant created in the H37Rv strain background was evaluated to confirm the role of *cya* in GSK2556286 resistance. The IC_{50} value in cholesterol media was >50 µM which is 25-fold higher than the IC_{50} value of the wild type strain. These results demonstrated that the *cya* gene has a role in resistance to GSK2556286 in *M. tuberculosis.*

Additional drug susceptibility testing of a selection of GSK2556286-resistant mutants (EM08, EM10, EM19, EM63) showed susceptibility to a selection of commonly used antitubercular drugs (Table 2, Supplemental Table S3) in axenic conditions but also showed susceptibility in an intra macrophage assay (Table 3).

Table 2. Antitubercular drug activity against selected GSK2556286-resistant *M. tuberculosis* strains. Data presented as the ratio of IC_{90} mutant/IC_{90} Wt EM01

Compound	**Strain**					
	EM05[b]	**EM08**[a]	**EM10**[a]	**EM19**[a]	**EM33**[b]	**EM63**[a]
Moxifloxacin	0.4	0.4	0.4	0.4	0.5	0.4
Linezolid	0.7	0.7	0.8	0.6	1.6	1.2
Pretomanid	0.8	0.8	0.9	1.1	1.5	1.3
Rifampicin	0.9	0.8	0.8	0.8	1.4	1.4
Bedaquiline	2.3	2.2	1.7	0.8	≤ 2.0	2.2
Ethionamide	1.2	1.5	0.9	1.3	1.8	1.0
Ethambutol	1.3	1.6	1.4	1.9	1.7	1.1
Kanamycin	0.4	0.4	0.5	0.5	0.4	0.8
Streptomycin	0.6	0.5	0.6	0.8	0.8	0.6
Amikacin	0.3	0.3	0.4	0.3	0.3	0.4
D-cycloserine	1.0	0.8	0.8	1.1	0.8	0.9
PAS	1.1	1.3	1.0	0.6	0.4	0.8

Key: [a] *cya* mutation ; [b] no *cya* mutation.

151 To be considered significant, the shift in activity ratio between resistant mutant and
152 laboratory strain (wt for cya) should be >4.

153

154 **Table 3**. Susceptibility of THP-1 infected with a selection of GSK2556286-resistant *M.*
155 *tuberculosis* strains to established antituberculars. Data presented as Ratio IC_{50} mutant/IC_{50}
156 wild type EM01

	Strain	
Compound	**EM19[a]**	**EM33[b]**
Isoniazid	0.57	0.54
Rifampicin	0.77	0.47
Moxifloxacin	0.32	0.30

157 Key: [a] *cya* mutation ; [b] no *cya* mutation.

158 To be considered significant, the shift in activity ratio between resistant mutant and
159 laboratory strain (wt for cya) should be >4.

160

161 Calculation of the spontaneous frequency of resistance has, to date, been technically
162 limited due to the challenging process of achieving acceptable growth in cholesterol-containing
163 solid culture media. Further efforts are ongoing to refine the methodology to enable accurate
164 assessments for spontaneous frequency of resistance to GSK2556286.

165

166 *Chemical and structural information and physicochemical properties*

167 GSK2556286A (Fig. 1) is a substituted 4-aryloxypiperidine with a low-to-moderate
168 molecular weight (MW=329.39).

169

170

Figure 1. Chemical structure of GSK2556286

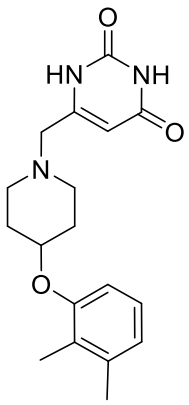

The white-to-slightly-colored solid is crystalline with a high melting point (200°C) and a chromatographic logD and Pharmaceutical Formulation Index (PFI) of 4.4 and 6.4, respectively. GSK2556286A has excellent stability in the solid and solution states with respect to temperature and light, giving confidence that a solid oral product with a suitable shelf life can be developed. GSK2556286 is practically insoluble in water, fasted state simulated intestinal fluid (FaSSIF), fed state simulated intestinal fluid (FeSSIF) and aqueous solution in a pH range of 5-9. It is very slightly soluble in simulated gastric fluid and aqueous solution in a pH range of 2-4.

The Developability Classification System (DCS) class (12) borders on IIa/b at the predicted dose, suggesting potential issues with solubility and dissolution at high doses (Figure S1).

Figure 2. Synthetic route

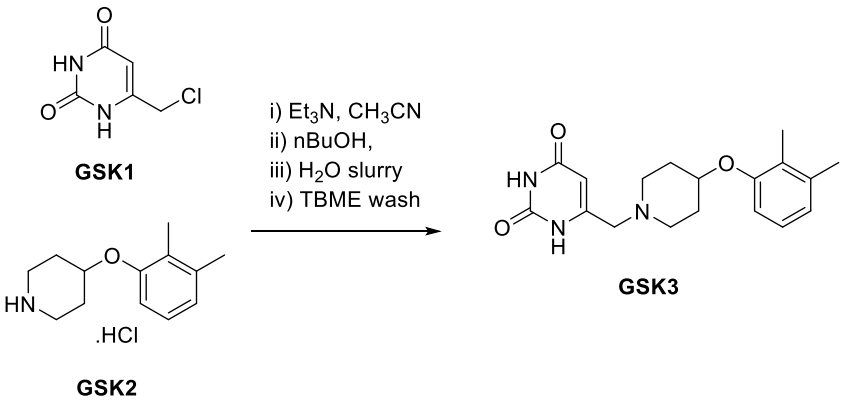

GSK2556286 was obtained in excellent yield in multi-gram scale trough a nucleophilic substitution of 6-(chloromethyl)-uracil derivative (GR202687X), and 4-(2,3-dimethylphenoxy)piperidine hydrochloride salt (GSK2422021A), both commercially available, catalyzed by triethylamine.

In vitro absorption, distribution, metabolism and elimination (ADME) and pharmacokinetic (DMPK) profiles and potential for drug-drug interactions

Physicochemical properties, *in vitro* ADME, and *in vivo* DMPK profiles in preclinical species (mouse, rat, dog) were evaluated to support progression of GSK2556286 and dose prediction modelling in humans. GSK2556286 displayed notably higher solubility in simulated gastric fluid compared to that in other biologically relevant media. The compound exhibited high passive permeability in the hMDR1-MDCK-II cell line, and although it was shown to be an in vitro substrate for P-glycoprotein, based on its permeability and existing *in vivo* preclinical pharmacokinetic data, permeability is not expected to limit oral absorption of GSK2556286 in humans. Low intrinsic clearance (CL_{int}) was determined in both human microsomes and hepatocytes. Low plasma protein binding (PPB) and low-to-moderate blood-to-plasma partitioning ratios (B/P) were observed in human and preclinical species (Supplemental Table S5).

Pharmacokinetics of GSK2556286 after intravenous and oral administration at various doses were evaluated in rodents and dogs. The compound exhibited low-to-moderate blood clearance, as predicted by CL_{int} in hepatocytes, and moderate volume of distribution. Absorption was rapid and oral bioavailability at pharmacologically relevant doses was high in mice and moderate in rats and dogs, in agreement with the expected first-pass effect (Supplemental Table S6)

Human PK parameters were calculated for GSK2556286 using a physiologically-based pharmacokinetic (PBPK) modelling approach (GastroPlus), based on physicopchemical, preclinical (in vitro and in vivo) and in vitro juman data. The PBPK models accurately predicted the IV and oral PK data from preclinical studies in mice, rats and dogs, and the prediction estimates a low human blood clearance (3.3 mL/min/kg), a moderate volume of distribution (3.5 L/kg) and high oral bioavailability (≥ 60% for predicted clinical doses). Taking as a reference the minimum AUC and C_{max} at 10 mg/kg associated with a maximum effect as a single drug in BALB/c mice, it was predicted a dose in humans between 150 and 300 mg/day administration (based on targeting AUC and C_{max}, respectively).

To assess the risk of drug-drug interactions, direct inhibition of CYP isoforms was investigated by assessing the enzyme activities (CYP1A2, CYP2C9, CYP2C19, CYP2D6 and CYP3A4) in an incubation mixture of microsomes with NADPH, in the presence and absence of GSK2556286. This preliminary evaluation showed that, although it did not substantially inhibit CYP1A2, 2C9, 2C19, 2D6 and 3A4 (IC50 values >25 µM), there is a moderate risk of CYP3A4-mediated perpetrator drug interactions assuming a CYP3A4 IC50 value of 25 µM and predicted human PK parameters for a 150 mg dose of GSK2556286. (Supplemental Table S7).

All studies were conducted in accordance with the GSK Policy on the Care, Welfare and Treatment of Laboratory Animals and were reviewed the Institutional Animal Care and Use Committee either at GSK or by the ethical review process at the institution where the work was performed.

Safety profile

GSK2556286 was evaluated in single dose oral toxicity studies in the rat, dog and cynomolgus monkey and in repeat dose oral toxicity studies of up to 4 weeks duration in the Wistar Han rat and cynomolgus monkey under GLP conditions and performed according to ICH guidelines. In addition, GSK2556286 was evaluated in a battery of *in vitro* and *in vivo* safety pharmacology (respiratory, cardiovascular and neurobehavioral tests) and genotoxicity

236 studies (including an Ames test on GSK2422021, a synthetic intermediate, predicted degradant
237 and a metabolite of GSK2556286).

238 In the definitive repeat dose oral toxicity studies in rat and monkey, adverse systemic
239 effects were limited to the rats in the high dose group (1000 mg/kg/day). No adverse effects
240 were observed at exposures up to an $AUC_{0\text{-}t}$=65.2 µg*h/mL and C_{max}= 5.89 µg/mL in male
241 and $AUC_{0\text{-}t}$=129 µg*h/mL and C_{max}=14.6 µg/mL in female rats and $AUC_{0\text{-}t}$=158 µg*h/mL and
242 mean C_{max}=9.96 µg/mL in the cynomolgus monkey (gender-averaged). GSK2556286 did not
243 produce acute cardiovascular effects in rat or monkey, respiratory effects in monkey or adverse
244 neurobehavioural effects in rats in single or repeat dose studies up to 1000 mg/kg/day and the
245 weight of evidence from *in vitro* and *in vivo* assessments indicates that GSK2556286 does not
246 present a genotoxic hazard to humans. The preclinical safety profile supports continued
247 progression to a first-time-in-humans (FTIH) trial.
248 All animal studies were ethically reviewed and carried out in accordance with Animals (Scientific
249 Procedures) Act 1986 and the GSK Policy on the Care, Welfare and Treatment of Animals.
250

251 *Efficacy in murine models of TB*

252 *Dose-ranging activity as monotherapy*

253 GSK2556286 was tested for *in vivo* efficacy in two different murine models of chronic
254 TB infection. In BALB/c mice, *M. tuberculosis* infection promotes development of
255 inflammatory cellular lung lesions in which *M. tuberculosis* resides virtually entirely
256 intracellularly, especially in macrophages, including foamy macrophages. In contrast,
257 C3HeB/FeJ mice also form caseating granulomatous lung lesions, in which *M. tuberculosis* is
258 found extracellularly in the acellular central caseum as well as inside neutrophils and
259 macrophages (13, 14).

The compound showed a statistically significant bactericidal effect when used as a single agent for 1 month (4 weeks) in chronic infection models in both mouse strains (Table 4). In BALB/c mice, all GSK2556286 doses tested were superior to no treatment ($p< 0.0001$) and the bactericidal effect was similar in magnitude to that of isoniazid. The maximal effect was achieved at a dose less than or equal to 10 mg/kg, which corresponded to a C_{max} of 1.38 ug/mL and an AUC_{last} of 6.61 µg*h/mL. In C3HeB/FeJ mice, all doses above 10 mg/kg were significantly better than no treatment ($p<0.05$) before adjustment for multiple comparisons, although only the 40 mg/kg dose was significantly different from no treatment after adjusting for multiple comparisons. Isoniazid was superior to each dose of GSK2556286 in C3HeB/FeJ mice ($p<0.01$).

Table 4. Lung CFU counts in BALB/c and C3HeB/FeJ mice after 4 weeks of GSK2556286 treatment

	Mean (± SD) lung CFU counts					
	BALB/c mice			**C3HeB/FeJ mice**		
Regimen	**Week -8**	**Day 0**	**Month 1**	**Week -8**	**Day 0**	**Month 1**
Untreated	1.95 ± 0.14	6.84 ± 0.23	6.71 ± 0.34	1.68 ± 0.10	7.00 ± 0.77	7.42 ± 0.95
INH (10 mg/kg)			5.54 ± 0.41*			4.93 ± 0.46*
GSK'286 (10 mg/kg)			5.63 ± 0.12*			6.52 ± 0.93
GSK'286 (40 mg/kg)			5.69 ± 0.05*			6.30 ± 0.54#
GSK'286 (100 mg/kg)			5.82 ± 0.08*			6.31 ± 1.00
GSK'286 (200 mg/kg)			5.50 ± 0.18*			6.30 ± 0.96

Key: *$p<0.01$ compared to untreated group. #$p<0.05$ compared to untreated group

GSK'286=GSK2556286

Contribution to bactericidal activity in combination therapy

Given the requirement for combination chemotherapy in the treatment of TB and the urgent need for novel regimens comprised of drugs that retain activity against MDR- and XDR-TB strains, the efficacy of GSK2556286 was evaluated in a subacute infection model in BALB/c mice that enables the evaluation of drug regimens against a higher bacterial burden (15). GSK2556286 (50 mg/kg) was co-administered with bedaquiline (B) and pretomanid (Pa) and the efficacy of this regimen was compared to that of BPa plus linezolid (L), which comprises a novel short-course regimen (16, 17) that was recently approved for treatment of XDR-TB and refractory MDR-TB. The addition of GSK2556286 to the BPa combination significantly increased efficacy, compared to BPa alone, after two months of treatment ($p<0.001$) (Table 5).

Table 5. Efficacy of GSK2556286 when combined with B and Pa in a BALB/c mouse model of TB. For comparison, the three-drug combination BPa+L is included

Regimen	**Mean lung log_{10} CFU (±SD)**		
	Day 0	**Month 1**	**Month 2**
Untreated	7.87 ± 0.12		
BPa		5.54 ± 0.32	3.17 ± 0.20
BPa+L		4.73 ± 0.28	0.73 ± 0.52
BPa+GSK2556286		5.39 ± 0.18	1.74 ± 0.76

Contribution to treatment-shortening activity in combination therapy

Although the bactericidal activity of this novel 3-drug combination was not as great as that of BPaL ($p<0.01$), the 6-log_{10} magnitude of the killing effect and clear contribution of GSK2556286 to the combination led us to assess the potential of GSK2556286 to contribute sterilizing activity when incorporated into 3- and 4-drug regimens with B, Pa and L in the subacute BALB/c mouse infection model, using the proportion of mice with relapse-free cure

297 as the primary endpoint. The standard of care RHZ (rifampicin+isoniazid+pyrazinamide) was
298 also included as reference for bactericidal outcome after 1 and 2 months of treatment and
299 relapse endpoint after 4 months based on previous data indicating RHZ requires more than 3
300 months to observe significant reductions in the proportion of mice that relapse (18, 19).

301 After 2 months of treatment, regimens combining GSK2556286 with BPa, BL or BPaL
302 resulted in significantly lower lung CFU counts compared to the first-line RHZ control
303 ($p<0.0001$, $p=0.0417$, and $p<0.0001$, respectively) (Table 6). BPa+GSK2556286 and
304 BPaL+GSK2556286 were not significantly different from BPaL at this time point, but
305 BL+GSK2556286 and PaL+GSK2556286 were significantly less active than BPaL
306 ($p<0.0001$). With respect to the relapse outcome, treatment with BPaL, BPa+GSK2556286 and
307 BPaL+GSK2556286 for 2 months resulted in lower proportions of mice relapsing compared to
308 treatment with RHZ for 4 months, indicating the treatment-shortening potential of regimens
309 combining GSK2556286 with BPa and BPaL, compared to RHZ. BL+GSK2556286 required
310 3 months of treatment to achieve a relapse rate lower than RHZ for 4 months.

311 The proportions of mice relapsing after 2 and 3 months of treatment with BPaL,
312 BPa+GSK2556286 and BPaL+GSK2556286 did not significantly differ, indicating that
313 GSK2556286 could replace L in the BPaL regimen without loss of efficacy. On the other hand,
314 PaL+GSK2556286 was associated with significantly more relapses ($p<0.0001$) at all time
315 points and BL+GSK2556286 was associated with more relapses ($p=0.0005$) after 2 months of
316 treatment but was similar after 3 and 4 months.

317

318

Table 6. Efficacy of GSK2556286 when combined with various 2- and 3-drug combinations of B, Pa and L in a BALB/c mouse model of TB.

	Mean lung log_{10} CFU (±SD)			Proportion of mice relapsing after treatment for:		
Regimen	**Day 0**	**Month 1**	**Month 2**	**2 months**	**3 months**	**4 months**
Untreated	7.30 ± 0.10					
RHZ		5.12±0.14	2.55±0.07	NT	NT	7/15
BPaL		3.10±0.17	0.00±0.00	4/15	1/15	NT
BPa+GSK2556286		3.77±0.36	0.27±0.54	5/15	1/15	0/15
BL+GSK2556286		4.16±0.34	1.91±0.33	14/15	2/14*	1/14*
PaL+GSK2556286		5.19±0.19	2.87±0.34	15/15	15/15	11/15
BPaL+GSK2556286		2.75±0.36	0.00±0.00	2/15	0/15	NT

Key: NT=Not tested. *, one of 15 mice died due to gavage accident and could not be assessed for relapse.

Activity in combination therapy in C3HeB/FeJ mouse model

These 3- and 4-drug regimens in which GSK2556286 was either added to BPaL or replaced B, Pa or L were also evaluated for CFU reduction in C3HeB/FeJ mice infected with *M. tuberculosis* H37Rv. After one month of treatment, none of these regimens was statistically significantly different from the RHZ or BPaL regimens (Figure 3). After two months, only PaL+GSK2556286 was significantly worse than RHZ (p=0.0006), suggesting GSK2556286 could replace either Pa or L in the BPaL regimen without loss of efficacy compared to BPaL or RHZ (group mean CFU counts are presented in Supplemental).

Figure 3. Efficacy of GSK2556286 (G) when combined with the various 2- and 3-drug combinations of B (bedaquiline), Pa (pretomanid) and L (linezolid) for 1 month (A) or 2 months (B) in a C3HeB/FeJ mouse model of TB. For comparison, B, BG and BPaL are included. Bars indicates median CFU counts. Median CFU on Day 0, the start of treatment, is indicated by dotted line.

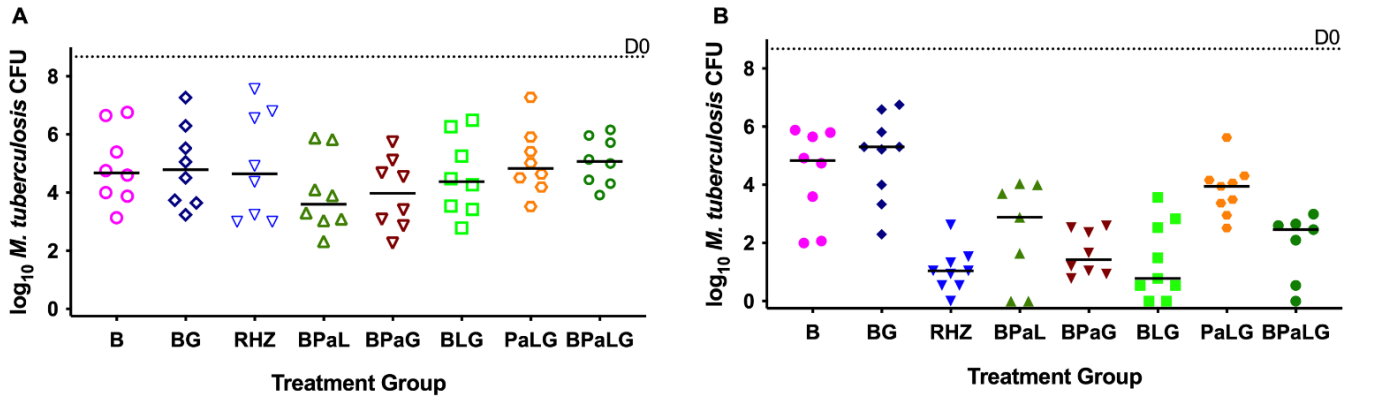

Discussion

GSK2556286 is a novel, small molecule, antitubercular compound identified from high-throughput intramacrophage screening that is active against a variety of drug-sensitive and drug-resistant clinical isolates in axenic culture in the presence of cholesterol as carbon source. Cholesterol uptake, catabolism and broader utilization are important for maintenance of the pathogen in the host, and other inhibitors of *M. tuberculosis* with activity revealed in the presence of cholesterol have been identified (9, 10, 11).

To further understand the potential cholesterol-dependent mode of action, GSK2556286-resistant *M. tuberculosis* clones were isolated on media containing cholesterol as the primary carbon source and analyzed by whole genome sequencing. Approximately half of the resistant clones sequenced harbored mutations in the gene for the membrane-anchored adenylyl cyclase, *cya,* without altering the viability of the bacteria at least in laboratory conditions. The observed frameshift and premature stop codon mutations indicated that loss of

351 *cya* function results in resistance to GSK2556286 and this was confirmed with the *cya*
352 knockout-mutant. These findings are similar to other recently discovered cholesterol-
353 dependent antitubercular leads that directly activate *cya* and induce bacterial cAMP production
354 and inhibit cholesterol production in wild type *M. tuberculosis* in an *cya*-dependent fashion [9].
355 Increased intracellular levels of cAMP, one of the main secondary messengers in the cell, may
356 negatively regulate cholesterol and propionate utilization by *M. tuberculosis*, reducing bacterial
357 growth when it is dependent upon utilizing these carbon sources (9, 20, 21). Therefore,
358 GSK2556286 may likewise act by activating *cya*, inducing cAMP production and negatively
359 regulating cholesterol and propionate utilization. Ongoing studies to further evaluate the mode
360 of action of GSK2556286, including its effects on cAMP levels and its impact in the presence
361 of cholesterol will be reported separately. Despite the need for further elucidation of the
362 specific mechanism of action, GSK2556286-resistant mutants remained susceptible to a list of
363 well-known antitubercular drugs that suggests the novelty of this mechanism.

364 Given that the macrophage is a major cellular niche for *M. tuberculosis*, blocking
365 replication of the bacterium in this environment may enhance existing or future TB drug
366 regimens (2, 6). However, human TB disease is also characterized by development of caseation
367 necrosis leading to closed caseous foci and cavities in which *M. tuberculosis* is found
368 extracellularly, in caseum. As caseum is also rich in cholesterol, those bacilli persisting
369 extracellularly in the acellular zones of caseous foci could also be susceptible to GSK2556286,
370 as they are in axenic culture in the presence of cholesterol (22, 23).

371 To demonstrate this therapeutic potential, GSK2556286 was evaluated, alone and in
372 combination with other drugs, in two murine TB models, one of which (C3HeB/FeJ mice) is
373 distinguished from other mouse models by its propensity to develop caseating lung lesions (24-
374 26). When used alone, GSK2556286 exhibited bactericidal effects in chronic infection models
375 in both BALB/c mice, where virtually all bacteria reside intracellularly, and in C3HeB/FeJ

mice, which form large caseating granulomas in which most bacteria are extracellular in caseum.

When used in combination to identify novel efficacious combination drug regimens including GSK2556286 in both models of TB, BALB/c and C3HeB/FeJ mice, GSK2556286 exhibited its potential to replace linezolid (L) in the BPaL regimen without loss of sterilizing activity. BPaL has been recently approved as a novel short-course oral treatment for XDR-TB and treatment refractory MDR-TB (27).

Although the individual contribution of GSK2556286 to the regimen's sterilizing activity was not shown directly in these studies, there was no loss of bactericidal or sterilizing activity of the BPaL regimen when GSK2556286 was substituted for linezolid in the BALB/c mouse infection model. The contribution of linezolid to the sterilizing activity of the BPaL regimen has been repeatedly demonstrated in this model (17) and thus these data suggest that GSK2556286 is likely to be contributing to the overall efficacy of the BPa+GSK2556286 regimen.

Furthermore, although there were more relapses after 2 and 3 months of treatment when GSK2556286 was substituted for Pa in BPaL (14 vs 4, and 2 vs 1, respectively), BL+GSK2556286 treatment for 3 and 4 months resulted in fewer relapses (2 and 1, respectively) than RHZ treatment for 4 months (7 relapses) in BALB/c mice and BL+GSK2556286 had bactericidal activity that could not be distinguished from RHZ or BPaL in C3HeB/FeJ mice.

In summary, GSK2556286 acts via a novel model of action to achieve significant in vivo activity in murine models displaying both cellular and extracellular lesion compartments. This result combined with the compound's low clearance values across a number of species, low propensity towards drug-drug interaction liabilities and adequate preliminary toxicology profile (genotoxicity, safety pharmacology, general toxicology) present evidence supporting

its progression as a new clinical candidate for the treatment of both MDR and drug-susceptible TB that has potential to contribute to the shortening of TB chemotherapy.

Materials and Methods

Microbiological assays. The MIC of GSK2556286 against extracellular *M. tuberculosis* laboratory strains was determined in standard media with glucose as a carbon source and also in media supplemented with cholesterol. For MIC determination in the absence of cholesterol, approximately $1x10^5$ CFU/mL of *M. tuberculosis* H37Rv (ATCC 25618) or Erdman (TMCC 107) was added to 96-well flat-bottom plates containing ten two-fold drug dilutions of GSK2556286 in Middlebrook 7H9 medium (Difco) supplemented with 2% glucose, 0.025% Tween 80, 0.05% Tyloxapol and 10% albumin-dextrose-catalase [ADC]). Plates were placed in a sealed box to prevent drying and incubated at 37°C for 6 days. 25 µL of Resazurin solution (38.6 µM) (Resazurin Tablets for Milk Testing; Ref 330884Y' VWR International Ltd, in 30 mL of phosphate buffered saline [PBS]) were added to each well. Fluorescence was measured after 48 hours at 37ºC using a SpectraMax M5 microplate reader (Molecular Devices). Non-linear regression analysis was used to fit the normalized fluorescence results into dose response curves and IC_{50} and IC_{90} values were determined using Excel Add-in XLFit. Reported data are the average of at least two experiments.

The MIC of GSK2556286 in media containing cholesterol as the carbon source was determined against *M. tuberculosis* H37Rv and Erdman strains with a final inoculum of approximately 1.4 $x10^6$ CFU/mL. Bacteria grown in 7H9 medium supplemented with 2% glucose and 0.025% Tyloxapol to an optical density (OD) around 0.5 at 600 nm were pelleted by centrifugation and washed twice with cholesterol media (Middlebrook 7H9 supplemented with 1 g/L KH_2PO_4, 2.5 g/L Na_2HPO_4, 0.5 g/L asparagine, 50 mg/L ferric ammonium citrate,

10 mg/L $MgSO_4 \cdot 7H_2O$, 0.5 mg/L $CaCl_2$, and 0.1 mg/L $ZnSO_4$ and 0.01% cholesterol as the sole carbon source). Pellets were resuspended in cholesterol media and incubated for at least 3 days at 37ºC. Plates containing GSK2556286 were inoculated and incubated at 37ºC for an additional 7 days, resazurin solution (38.6 μM) was added and incubated for 48 hours before fluorescence was measured. Rifampicin (Sigma R3501) was used as positive control up to 0.36 μM. IC_{50} and IC_{90} values were determined as described above. Reported data are the average of at least two experiments.

The intracellular antibacterial activity of GSK2556286 was determined using human THP-1 cells maintained in RPMI-1640 media containing 10% fetal bovine serum (FBS), 1mM of pyruvate, and 2mM of L-glutamine, and incubated at 37 ºC with 5% CO_2. An *M. tuberculosis* H37Rv reporter strain carrying the firefly luciferase gene (under the control of the *hsp60* promoter) was grown in Middlebrook 7H9 broth supplemented with 10% ADC, 0.4% glycerol and 0.05% Tween 80 until the mid-log phase. THP-1 cells were infected at a multiplicity of infection (MOI) of 1:1 in antibiotic-free RPMI-1640 media containing 10% FBS, 1 mM of pyruvate, 2 mM of L-glutamine and 20 nM of phorbol 12-myristate 13-acetate (PMA) for 4 hours at 37ºC with 5% CO_2. Following a 4-hour incubation period, infected cells were harvested and plated onto 96-well plates containing either GSK2556286 (up to 25 μM), rifampicin up to 0.73 μM as positive control, or dimethyl sulfoxide (DMSO) (<0.5% final concentration). After 5 days of incubation, cell luminescence was measured using the Bright-Glo Promega kit and SpectraMax M5 plate reader. The percentages of inhibition were calculated relative to the DMSO control well. For each compound, the average value of the duplicate samples was calculated, and a sigmoidal dose-response (variable slope) curve was fit by nonlinear regression (GraphPad) to enable estimation of the IC_{50}.

MIC determination against a panel of clinical isolates on cholesterol-based media. The MIC of GSK2556286 was determined against 45 clinical isolates of *M. tuberculosis* with different resistance phenotypes maintained by the National Institutes of Health. *M. tuberculosis* strains HN878, CDC1551, Erdman and H37Rv were included as controls. Individual *M. africanum* and *M. bovis* isolates were included to represent other members of the *M. tuberculosis* complex. Briefly, bacteria were grown to an OD of 0.2-0.6 in the 7H9 medium supplemented with bovine serum albumin, Tyoxapol and cholesterol as a sole carbon source and added (2 x 10^4 bacteria per well) to 96-well plates containing GSK2556286 (in concentrations ranging up to 50 μM). Para-aminosalicylic acid (PAS), isoniazid, and bedaquiline were used as positive controls and DMSO as a negative control. Plates were incubated for up to 3 weeks at 37°C. At various time points, plates were read with an inverted enlarging mirror plate reader and graded as either growth or no growth to determine the MIC. The time point was dependent on the growth rate of the strain in the drug-free control medium (generally between 1-2 weeks). After 2 weeks of incubation, resazurin was added to plates. Following incubation at 37°C for 24 hours, results were read visually with an inverted enlarging mirror plate reader (blue = growth inhibition, pink= growth). The lowest concentration to inhibit growth was defined as the MIC.

Selection of GSK2556286 resistant mutants in vitro. The MIC of GSK2556286 in cholesterol-containing agar medium was used to establish the concentration of GSK2556286 for the selection of resistant mutants. Stocks of *M. tuberculosis* Erdman (2x10^9 CFU/mL) were thawed and diluted 1:5 in PBS, and 0.1 mL aliquots were plated on 7H11 agar media containing cholesterol or cholesterol plus dextrose as carbon sources, with or without GSK2556286 at 96 μM (8xMIC). The bacterial colonies were counted after 4 or 6 weeks of incubation.

For genetic characterization, genomic DNA from single colonies was extracted with the MasterPureTM DNA Purification Kit from Epicentre (Cat. No. MCD85201) according to

the manufacturer's instructions. DNA libraries were generated following the Nextera XT Illumina protocol (Nextera XT Library Prep kit (FC-131-1024)). 0.2ng/ul purified gDNA was used to initiate the protocol. The multiplexing step was performed using Nextera XT Index Kit (FC-131-1096). The libraries were sequenced using a 2x150pb paired-end run, NextSeq high output reagent kit on a NextSeq Sequencer according to manufacturer's instructions (Illumina). Quality assessment was performed using prinseq-lite program (28) applying following parameters: Min_length: 50, Trim_qual_right: 20, Trim_qual_type: mean and Trim_qual_window: 20. R1 and R2 from Illumina sequencing where joined using fastq-join from ea-tools suite (29).

Creation of Rv1625c knock-out mutant. A knock-out mutant was created in the H37Rv strain by replacing *Rv1625c* with a hygromycin resistance cassette using the recombineering approach developed by Murphy et al (30). Gene replacement was confirmed by PCR.

Selection of GSK2556286-resistant mutants in vivo. C3HeB/FeJ mice received a low-dose aerosol infection with 31 CFU/ lung of *M. tuberculosis* Erdman. Starting 8 weeks post-infection, mice were given oral doses of GSK2556286 at 100 mg/kg, 5 days a week for 6 weeks. Lungs were harvested and homogenates were prepared and plated in serial 10-fold dilutions on plates with and without GSK2556286 at 100 μM.

Mouse efficacy studies

All housing and procedures involving mice were approved by the Institutional Animal Care and Use Committee at Johns Hopkins University School of Medicine and the GSK Policy on the Care, Welfare and Treatment of Animals.

Mice. Female specific pathogen-free BALB/c mice and C3HeB/FeJ mice, each aged 5-6 weeks, were purchased from Charles River (Wilmington, MA) and Jackson Laboratories (Bar Harbor, ME), respectively. Mice were housed in a bio-safety level 3 animal facility.

Mycobacterial Strain. *M. tuberculosis* H37Rv was mouse-passaged, frozen in aliquots and sub-cultured in Middlebrook 7H9 broth with 10% oleic acid-albumin-dextrose-catalase (OADC) (Fisher, Pittsburgh, PA) and 0.05% Tween 80 prior to infection.

Infection. BALB/c and C3HeB/FeJ mice were infected with *M. tuberculosis* H37Rv, using the Inhalation Exposure System (Glas-col, Terre Haute, IN). The chronic infection model in both mouse strains was initiated with a thawed aliquot of the bacterial culture that was diluted 1:50 with sterile PBS for infecting BALB/c mice and 1:100 for infecting C3HeB/FeJ mice with the goal of implanting approximately 100 and 50-75 CFU, respectively, in the lungs. Mice were held for 6 weeks before beginning treatment. The subacute infection model in BALB/c mice was initiated with a late log-phase culture in 7H9 broth (optical density at 600 nm of 0.8-1) with the goal of implanting 3.5-4 $\log_{10}$ CFU. Mice were held for 2 weeks before beginning treatment.

Drug treatments. For dose-ranging monotherapy studies, GSK2556286 in doses of 10, 40, 100 and 200 mg/kg body weight was formulated in 1% methylcellulose and isoniazid 10 mg/kg was prepared in distilled water. Drugs were administered orally via gavage once daily, five days per week, for four weeks. Positive and negative controls received isoniazid and no treatment, respectively.

For experiments evaluating the activity of GSK2556286 in combinations with bedaquiline, pretomanid and linezolid, GSK2556286 and isoniazid were formulated as described above. Other drugs were formulated and administered at the indicated dose as previously described (16, 17): rifampicin (10 mg/kg) and pyrazinamide (150 mg/kg) in distilled water, bedaquiline

(25 mg/kg) in acidified 10% (2-Hydroxypropyl)-ß-cyclodextrin (HPCD) solution, pretomanid (100 mg/kg) in 20% HPCD and lecithin (CM-2) formulation and linezolid (100 mg/kg) in 0.5% methylcellulose.

Assessment of efficacy. Two microbiological outcomes were assessed: lung CFU counts during treatment and the proportion of mice relapsing after completion of treatment. Lungs were collected and homogenized in glass grinders at pre-specified time points during and after drug treatment. The homogenates were serially diluted in PBS and plated on Middlebrook 7H11 agar plates supplemented with 10% (v/v) OADC (GIBCO) and cycloheximide [10 mg/mL], carbenicillin [50 mg/mL], polymixin B [25 mg/mL] and trimethoprim [20 mg/mL]. Homogenates from mice receiving drug combinations were plated on the same agar media but with the addition of activated charcoal powder (0.4%w/v) to prevent carryover of bedaquiline. Colonies were counted after 4 and 6 weeks of incubation at 37°C to ensure all cultivable bacteria would be detected. Relapse after 2, 3 and 4 months of treatment with drug combinations was assessed by holding cohorts of 15 mice per group for an additional 3 months without treatment before sacrificing the mice and plating the entire lung homogenate, as described above. Relapse was defined by detection of ≥ 1 CFU.

Statistical analysis. CFU counts (x) were log-transformed (as x+1) before analysis. Group means were compared by one-way analysis of variance with Dunnett's post-test to control for multiple comparisons. Group relapse proportions were compared using Fisher's exact test, adjusting for multiple comparisons. The Kruskal-Wallis test and Dunn's non-parametric post-test to adjust for multiple comparisons were used to test for significance on non-normally distributed CFU data from C3HeB/FeJ mice. GraphPad Prism version 6 (GraphPad, San Diego, CA) was used for all analyses. Use of 15 mice per group for relapse assessment provides approximately 80% power to detect 40 percentage point differences in the relapse rate, after

setting alpha at 0.01 to adjust for up to 5 simultaneous two-sided comparisons. Smaller differences may not be meaningful in terms of shortening the duration of treatment.

Data will be made publicly available upon publication and upon request for peer review.

Acknowledgments: We would like to thank to Kevin Pethe and Jichan Jang for their collaboration with the screening at Institute Pasteur Korea. We would like to thank Ken Duncan and Peter Warner from the Bill & Melinda Gates Foundation, Steve Berthel from the New Venture Fund, and GSK technical and administrative support staff. We would like to thank Dirk Schanppinger and Curtiss Engelhart for providing KO strain and Anne Lenaerts for assistance with the in vitro and *in vivo* selection of resistant mutants.

Funding: This work was funded, in part, by a Tres Cantos Open Lab Foundation (grant number TC049), by the European Union's 7th framework program (FP7- 2007-2013) under the Orchid grant agreement No. 261378 and in part by the Division of Intramural Research of the NIAID/ NIH This work was supported, in whole or in part, by the Bill & Melinda Gates Foundation [OPP1178195.]. Under the grant conditions of the Foundation, a Creative Commons Attribution 4.0 Generic License has already been assigned to the Author Accepted Manuscript version that might arise from this submission.

References

1. Global Tuberculosis Report 2020. World Health Organization, 2020. Geneva.
2. Cole ST. 2016. Inhibiting *Mycobacterium tuberculosis* within and without. Philos Trans R Soc Lond B Biol Sci 371. 2016 Nov 5;371(1707):20150506. doi: 10.1098/rstb.2015.0506
3. Kushner S, Dalalian D, Sanjurjo JL, Bach Jr. FL, Safir SR, Smith Jr. VK, Williams JH. 1952. Experimental Chemotherapy of Tuberculosis. II. The Synthesis of Pyrazinamides and Related Compounds. J Am Chem Soc 74:3617-3621.
4. Malone L, Schurr A, Lindh H, Mc KD, Kiser JS, Williams JH. 1952. The effect of pyrazinamide (aldinamide) on experimental tuberculosis in mice. Am Rev Tuberc 65:511-8.
5. Parish T. 2020. In vitro drug discovery models for *Mycobacterium tuberculosis* relevant for host infection. Expert Opin Drug Discov 15:349-358.
6. Christophe T, Jackson M, Jeon HK, Fenistein D, Contreras-Dominguez M, Kim J, Genovesio A, Carralot JP, Ewann F, Kim EH, Lee SY, Kang S, Seo MJ, Park EJ, Skovierova H, Pham H, Riccardi G, Nam JY, Marsollier L, Kempf M, Joly-Guillou ML, Oh T, Shin WK, No Z, Nehrbass U, Brosch R, Cole ST, Brodin P. 2009. High content screening identifies decaprenyl-phosphoribose 2' epimerase as a target for intracellular antimycobacterial inhibitors. PLoS Pathog 5:e1000645.
7. de Jager VR, Dawson R, van Niekerk C, Hutchings J, Kim J, Vanker N, van der Merwe L, Choi J, Nam K, Diacon AH. 2020. Telacebec (Q203), a New Antituberculosis Agent. N Engl J Med 382:1280-1281.
8. Pethe K, Bifani P, Jang J, Kang S, Park S, Ahn S, Jiricek J, Jung J, Jeon HK, Cechetto J, Christophe T, Lee H, Kempf M, Jackson M, Lenaerts AJ, Pham H, Jones V, Seo

MJ, Kim YM, Seo M, Seo JJ, Park D, Ko Y, Choi I, Kim R, Kim SY, Lim S, Yim S-A, Nam J, Kang H, Kwon H, Oh C-T, Cho Y, Jang Y, Kim J, Chua A, Tan BH, Nanjundappa MB, Rao SPS, Barnes WS, Wintjens R, Walker JR, Alonso S, Lee S, Kim J, Oh S, Oh T, Nehrbass U, Han S-J, No Z, et al. 2013. Discovery of Q203, a potent clinical candidate for the treatment of tuberculosis. Nature Medicine 19:1157.

9. VanderVen BC, Fahey RJ, Lee W, Liu Y, Abramovitch RB, Memmott C, Crowe AM, Eltis LD, Perola E, Deininger DD, Wang T, Locher CP, Russell DG. 2015. Novel inhibitors of cholesterol degradation in *Mycobacterium tuberculosis* reveal how the bacterium's metabolism is constrained by the intracellular environment. PLoS Pathog 11:e1004679.

10. Pandey AK, Sassetti CM. 2008. Mycobacterial persistence requires the utilization of host cholesterol. Proc Natl Acad Sci U S A 105:4376-80.

11. LeeW, Vanderven BC, Fahey RJ, Russell DG. Intracellular Mycobacterium tuberculosis exploits host-derived fatty acids to limit metabolic stress. The Journal of Biological Chemistry, 10 Jan 2013, 288(10):6788-6800.
DOI: 10.1074/jbc.m112.445056

12. Rosenberger J, Butler J, Dressman J. 2018. A Refined Developability Classification System. J Pharm Sci 107:2020-2032.

13. Rosenthal IM, Tasneen R, Peloquin CA, Zhang M, Almeida D, Mdluli KE, Karakousis PC, Grosset JH, Nuermberger EL. 2012. Dose-ranging comparison of rifampin and rifapentine in two pathologically distinct murine models of tuberculosis. Antimicrob Agents Chemother 56:4331-40.Driver ER, Ryan GJ, Hoff DR,

14. Irwin SM, Basaraba RJ, Kramnik I, Lenaerts AJ. 2012. Evaluation of a mouse model of necrotic granuloma formation using C3HeB/FeJ mice for testing of drugs against *Mycobacterium tuberculosis*. Antimicrob Agents Chemother 56:3181-95.

15. Nuermberger EL. 2017. Preclinical Efficacy Testing of New Drug Candidates. Tuberculosis and the Tubercle Bacillus 2nd Edition (CH 13; pp. 269-293) ISBN:9781555819552. DOI:10.1128/9781555819569.ch13.

16. Conradie F, Diacon AH, Ngubane N, Howell P, Everitt D, Crook AM, Mendel CM, Egizi E, Moreira J, Timm J, McHugh TD, Wills GH, Bateson A, Hunt R, Van Niekerk C, Li M, Olugbosi M, Spigelman M. 2020. Treatment of Highly Drug-Resistant Pulmonary Tuberculosis. N Engl J Med 382:893-902.

17. Tasneen R, Betoudji F, Tyagi S, Li SY, Williams K, Converse PJ, Dartois V, Yang T, Mendel CM, Mdluli KE, Nuermberger EL. 2016. Contribution of Oxazolidinones to the Efficacy of Novel Regimens Containing Bedaquiline and Pretomanid in a Mouse Model of Tuberculosis. Antimicrob Agents Chemother 60:270-7.

18. Li SY, Tasneen R, Tyagi S, Soni H, Converse PJ, Mdluli K, Nuermberger EL. 2017. Bactericidal and Sterilizing Activity of a Novel Regimen with Bedaquiline, Pretomanid, Moxifloxacin, and Pyrazinamide in a Murine Model of Tuberculosis. Antimicrob Agents Chemother 61.

19. Williams K, Minkowski A, Amoabeng O, Peloquin CA, Taylor D, Andries K, Wallis RS, Mdluli KE, Nuermberger EL. 2012. Sterilizing activities of novel combinations lacking first- and second-line drugs in a murine model of tuberculosis. Antimicrob Agents Chemother 56:3114-20.

20. Johnson RM, Bai G, DeMott CM, Banavali NK, Montague CR, Moon C, Shekhtman A, VanderVen B, McDonough KA. 2017. Chemical activation of adenylyl cyclase Rv1625c inhibits growth of *Mycobacterium tuberculosis* on cholesterol and modulates intramacrophage signaling. Mol Microbiol 105:294-308.

21. Bonds AC, Sampson NS. 2018. More than cholesterol catabolism: regulatory vulnerabilities in *Mycobacterium tuberculosis*. Curr Opin Chem Biol 44:39-46.

641 22. Sarathy JP, Dartois V. 2020. Caseum: a Niche for *Mycobacterium tuberculosis* Drug-
642 Tolerant Persisters. Clin Microbiol Rev 33.
643 23. Caseation of human tuberculosis granulomas correlates with elevated host lipid
644 metabolism**.**
645 Kim MJ1, Wainwright HC, Locketz M, Bekker LG, Walther GB, Dittrich C, Visser
646 A, Wang W, Hsu FF, Wiehart U, Tsenova L, Kaplan G, Russell DG. EMBO
647 Molecular Medicine, 01 Jul 2010, 2(7):258-274
648 DOI: 10.1002/emmm.201000079
649 24. Irwin SM, Driver E, Lyon E, Schrupp C, Ryan G, Gonzalez-Juarrero M, Basaraba RJ,
650 Nuermberger EL, Lenaerts AJ. 2015. Presence of multiple lesion types with vastly
651 different microenvironments in C3HeB/FeJ mice following aerosol infection with
652 Mycobacterium tuberculosis. Dis Model Mech 8:591-602.
653 25. Lanoix JP, Lenaerts AJ, Nuermberger EL. 2015. Heterogeneous disease progression
654 and treatment response in a C3HeB/FeJ mouse model of tuberculosis. Dis Model
655 Mech 8:603-10.
656 26. Pan H, Yan BS, Rojas M, Shebzukhov YV, Zhou H, Kobzik L, Higgins DE, Daly MJ,
657 Bloom BR, Kramnik I. 2005. Ipr1 gene mediates innate immunity to tuberculosis.
658 Nature 434:767-72.
659 27. Haley CA, Macias P, Jasuja S, Jones BA, Rowlinson M-C, Jaimon R, Onderki P,
660 Darnall E, Gomez ME, Peloquin C, Ashkin D, Goswami ND. Novel 6-month
661 Treatment for Drug-Resistnat Tuberculosis, US. Emerg Infect Dis. 2021;27(1):332-
662 334
663 28. Schmieder, R. and Edwards, R. (2011). Quality control and preprocessing of
664 metagenomic datasets. 97 Bioinformatics, 27(6):863–864.

665 29. Aronesty E. ea-utils: Command-line tools for processing biological sequencing data.
666 January 2011 Expression Analysis.
667 30. Murphy KC, Campellone KG. Lambda Red-mediated recombinogenic engineering of
668 enterohemorrhagic and enteropathogenic *E. coli*. *BMC Mol Biol.* 2003;4:11

669